Supplementary Materials

Evaluation of EXaCT-2 on a diverse cohort of cancers

To illustrate the diversity of the samples we here report the distribution of samples by site of origin for all the matched cases in the Discovery Cohort (n=244), including 106 primary cancers, 31 metastatic cancers, and 107 organoids/xenografts (Figure S1).

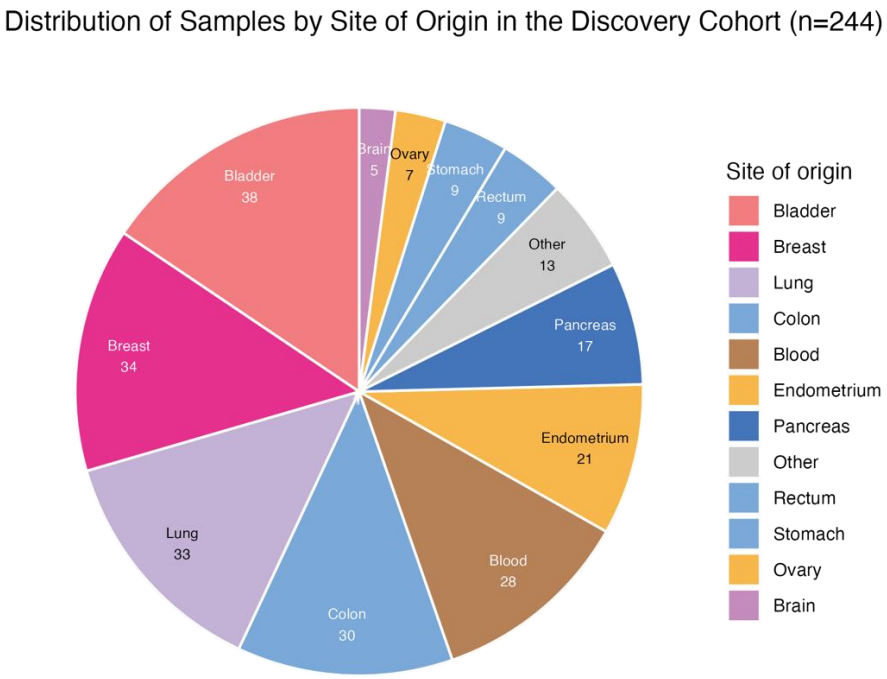

Figure S1: *Pie chart illustrating the percentage of the cases by site of origin. The Discovery Cohort includes 106 primary cancers, 31 metastatic cancers, and 107 organoids/xenografts.*

Enhanced precision in detecting boundaries of somatic copy number alterations (SCNAs)

To explore the advantages that the expanded set of probes provide to the identification of SCNAs, we leveraged the 4 cases that were analyzed by both EXaCT-1 and EXaCT-2. First, to ensure that both assays produced similar results for these co-analyzed cases, we first performed a gene-wise comparison of the results from the analysis from each assay (Table S3) and determined that the results were statistically similar (Chi-Square $p < 0.00001$).

Second, we observed that the total fraction of the genome altered (FGA) by an SCNA was nearly unchanged between the two assays ($p=0.59$; Figure S2A, Table S4). In contrast, however, the total number of inferred segments was considerably higher in the results from the EXaCT-2 assay, indicating that the EXaCT-2 assay might provide for finer granularity of the segmentation generated by the SCNA analysis ($p=0.056$; Figure 2C-Top, Table S5). To further examine this hypothesis, the segments generated from the two assays were stratified by segment length and compared. While there was no statistical difference between the mid-sized segments (those between 25-100Mb), the EXaCT-2 assay produced significantly fewer large (>100MB) and small segments (<25Mb), indicating that the EXaCT-1 segments were both over- and under-segmented, in comparison to those from the EXaCT-2 assay (Figure S2B).

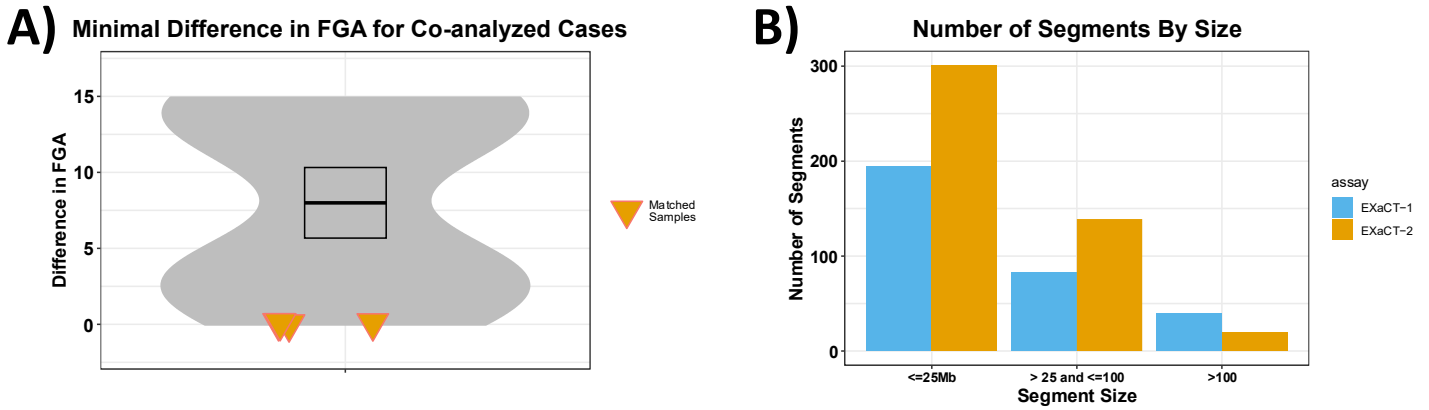

***Figure S2** Comparison and analysis of SCNA segments across four cases profiled by 2 WES assays. **A)** Difference in the total Fraction of Genome Altered (FGA): No major difference is observed in FGA between matching EXaCT-1 and EXaCT-2 samples; co-analyzed cases are highlighted and compared against a simulated null that was generated by calculating the difference for all possible pairwise comparisons of the samples. **B)** Grouping segments based on their size: As number of segments suggest, EXaCT-2 shows a higher prevalence of smaller segments (<25Mb) and lower number of larger segments (>100 Mb) compared to EXaCT-1.*

Given these results, we performed a systematic analysis and comparison of the segmentations generated by the two assays (Figure S3). We first evaluated the number of segments identified by both assays, as well as those which were unique to each assay. When using an extremely simplified definition of concordance as being any region in one assay where at least half of it overlapped with one or more regions from the other assay, we discovered that on average 98.1% of all segments from EXaCT-1 overlapped with those identified in EXaCT-2, and 95.8% of all EXaCT-2 segments overlapped with those identified with EXaCT-1 (see Methods for details on how SCNAs were identified for each assay). Even when using a more stringent threshold by requiring 95% overlap between the segments, these proportions only drop to 87.8% and 89.0%, respectively. Note, that with this simplified definition of concordance, we do not consider inferred copy number for reasons that we will discuss further below.

By using these overlapping regions, we next sought to identify the number segments that were mutually and uniquely identified by both assays, meaning segments from one assay that mutually and uniquely overlapped segments from the other assay. We further limited these matches to those where the overlap between the 2 segments was at least 80% for at least one segment, and they had concordant copy number rations (both concordantly showed amplification or deletion, even if insignificantly). Given this definition of concordance, the overall average number of matching segments was 23.5. However, with a standard deviation of 28.8, these results indicated a high variability in the number of matching segments.

This high variability resulted from 2 samples that had almost no shared segments (n <=1 for both). For both samples, the EXaCT-2 segmentation had nearly twice the number of segments from the EXaCT-1 segmentation, or higher, indicating that the EXaCT-1 assay led to an under-segmentation of these samples. Some caution should be taken, given the small sample sizes, but even when these 2 samples were excluded, the average number of shared segments was 46.5, with a standard deviation of 19.1, which still represents a small number of segments for either assay for the remaining 2 samples.

Given these indications of under-segmentation from the analyses with EXaCT-1, we next sought to explore and quantify the degree of under- or over-segmentation from either assay. To do this, we first introduce a couple of terms. We define an **oversized (undersegmented) segment** as any segment from one assay that overlaps with more than one segment from the other. Conversely, we define a **split segment** as a segment from one assay that, along with other adjacent split segments, overlaps with an oversized segment from the other assay (Figure S3A).

A)

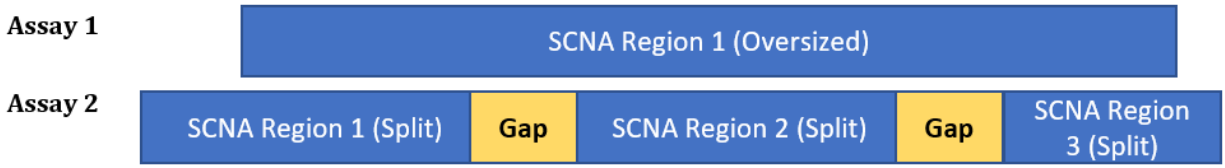

B)

	EXaCT-2	EXaCT-1
Total number of Oversized Regions	56	102
Number of Missed Events	24	22

C)

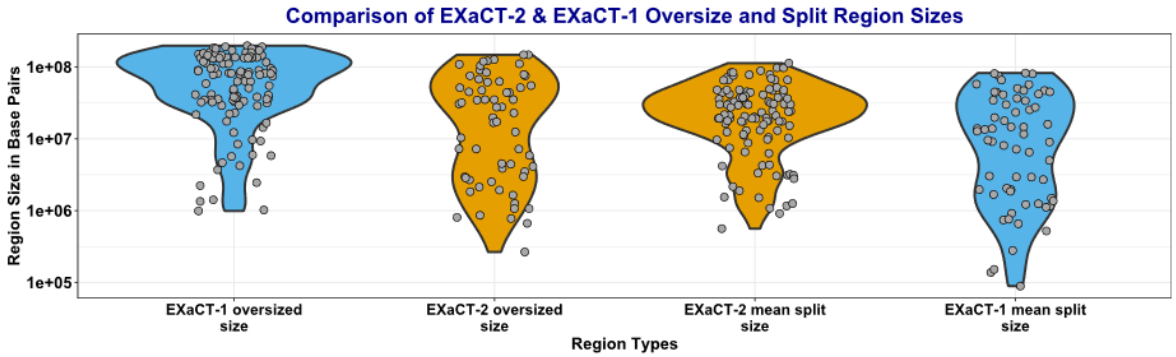

D)

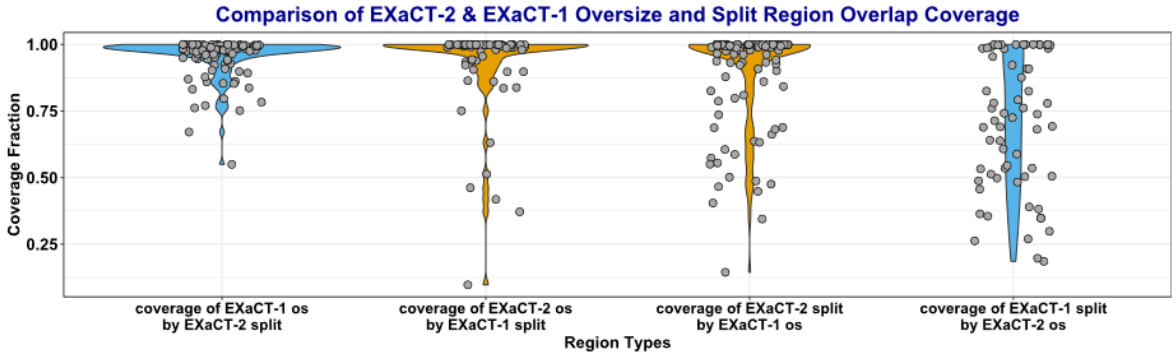

Figure S3 *A) Schematic of the oversized regions from one assay, and the split regions from the results of the other, where in a given region Assays 1 and 2 identify somatic copy number alterations and segments, but Assay 1 has generated a region that was decomposed into smaller regions by Assay 2.* ***B)*** *A comparison of the total number of oversized regions for EXaCT-1 and EXaCT-2 identified in the matching 4 cases, along with the total number of discordant events (SCNA events that were identified in the results from one assay but not identified in the results of the other assay).* ***C)*** *Comparison of the sizes of the* ***oversized*** *and* ***split*** *regions from the EXaCT-1 and EXaCT-2 regions.* ***D)*** *Comparison of the reciprocal overlapping coverage of the* ***oversized*** *and* ***split*** *regions from the 2 assays.*

Overall, we observed that the number of oversized EXaCT-1 regions was significantly greater than the number of oversized EXaCT-2 regions (p=0.042). Likewise, the number of EXaCT-2 split regions was also significantly greater than the number of EXaCT-1 split regions (p=2.25e-8). This was also reflected in the average size of these regions (Figure S3B), where the EXaCT-1 oversized regions were significantly larger than the EXaCT-2 oversized regions (p=4.51e-7), while there was no statistical difference in the size of the EXaCT-2 oversized and split regions (p=0.15). We also noticed that the EXaCT-1 split regions were significantly smaller than any of the others (p=7.26e-4 when compared with all of the EXaCT-2 regions - Figure S3C). We also were struck by the reciprocal overlap of the oversized and split regions, e.g. how much of an oversized EXaCT-1 region overlaps with split regions from the EXaCT-2 assay, and vice versa (Figure S3C). With the exception of the EXaCT-1 split regions, the median overlap was 0.99.

In Figure S3D, we demonstrate that the oversized regions from EXaCT-1 are nearly perfectly covered by their respective split regions from the EXaCT-2 assay. Similarly, we demonstrate that the EXaCT-2 oversized regions are nearly perfectly covered by their corresponding EXaCT-1 split regions, however, the converse is not true. Instead, the EXaCT-1 split regions are significantly less well-aligned and less concordant than the results from EXaCT-2.

Comparing SCNA between EXaCT-1 and EXaCT-2

To assess the SCNA between EXaCT-1 and EXaCT-2, a set of four samples profiled by the two assays was selected and compared based on various factors such as Total Fraction Genome Altered (FGA), the total number of segments, and the size of the segments.

FGA: To determine the Total Fraction of genome altered (FGA) in a sample, the sum of the total number of bases with Copy No. Loss or Gain is divided by the total number of bases targeted by EXaCT-2.

Total Number of Segments: When counting the total number of segments, all segments regardless of their copy number status from EXaCT-1 were considered, which were identified using the DNACopy, as previously described [1,2]. Similarly, the total number of segments from EXaCT-2 encompassed all segments, irrespective of copy number status, obtained from tool CNVKit.

Size of segments: To evaluate the segment size and resolution of copy number segments between EXaCT-1 and EXaCT-2, the segments were categorized into three groups: small segments (<25Mb), mid-sized segments (>25MB and <100Mb), and large segments (>100Mb). The distribution of segments across these three categories was then analyzed.

SCNA Gene Concordance

To evaluate the concordance of SCNA and assess the similarity between EXaCT-1 and EXaCT-2 assays, we calculated Gene-Level Concordance for the four corresponding samples. The log2 ratio across each of the 20,000 genes was compared between the matched samples from EXaCT-1 and EXaCT-2. Subsequently, the absolute difference in log2 ratio for each gene between EXaCT-1 and EXaCT-2 matching samples was determined. To mitigate the impact of noisy SCNA calls, a smoothing factor of 0.3 was applied to the absolute difference in log2 ratio. If the absolute difference was less than or equal to 0.3, an average of the log2 ratio for that gene from EXaCT-1 and EXaCT-2 was computed. If the absolute difference exceeded 0.3, the original log2 values for the genes were retained. Following this, genes were categorized into different types of SCNA Events (Copy No. Gain or Copy No. Loss or Neutral) based on a predefined threshold.

Fusions

Figure S4 illustrates the broad spectrum of known fusions that have at least one breakpoint in the non-coding regions that are targeted by the EXaCT-2 assay.

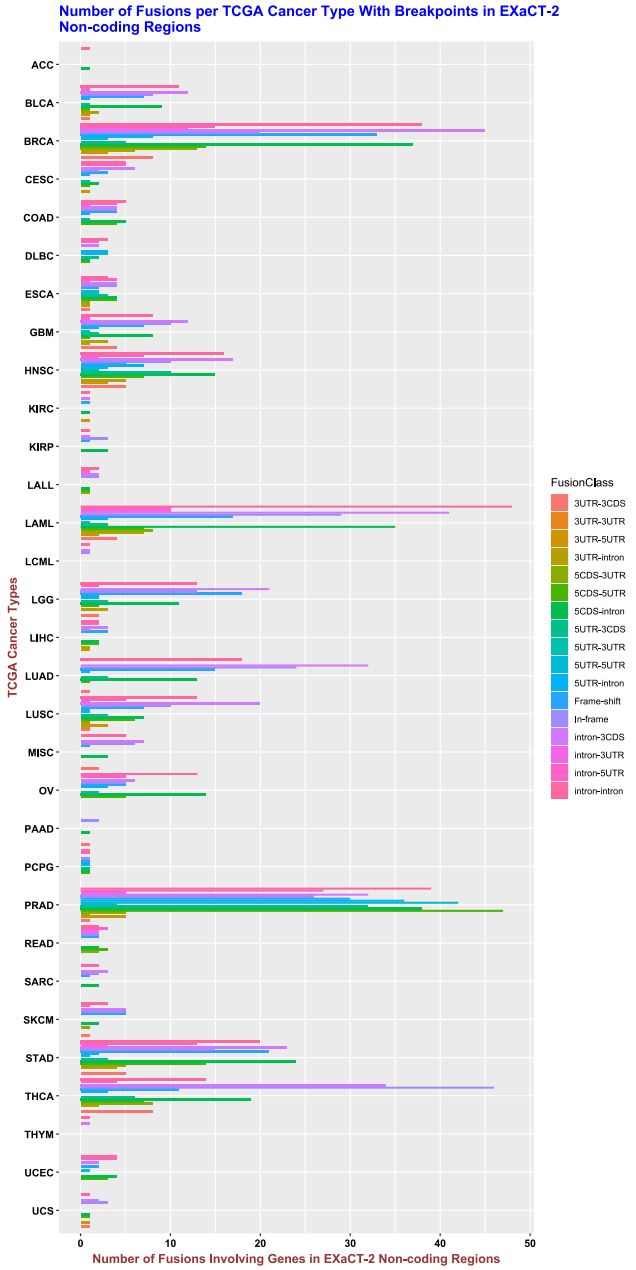

Figure S4: Broad Spectrum of Fusions Targeted by EXaCT–2. *Fusions are separated by cancer type (using TCGA acronyms) and fusion class, as defined by the source that provided the list of fusions. This list of fusions was downloaded from FusionGDB v.2.0 [3], and limited to those which have at least one (1) breakpoint that occurs in the non-coding regions that are targeted by the EXaCT-2 assay. To prevent double-counting fusions, we define those that share the same breakpoints (same chromosomal coordinates for both breakpoint1 and breakpoint2) as being duplicate fusions, and limit the set to only including one representative of that fusion.*

NTRK2-KANK2 Rearrangement

As negative controls, we used 2 samples that were identified to possess fusions involving Neurotrophic Receptor Tyrosine Kinase 2 (NTRK2—KANK2 and NTRK2—AFAP1), as none of the genes involved in these fusions were included in the set of 66 genes that were targeted for fusion detection, as described above. EXaCT-2 was able to recover the NTRK2-KANK2 fusion as the breakpoint for the KANK2 gene occurred in the exon padding region on the 3’ side of the fourth exon (Tables S8-9 and Figure S5).

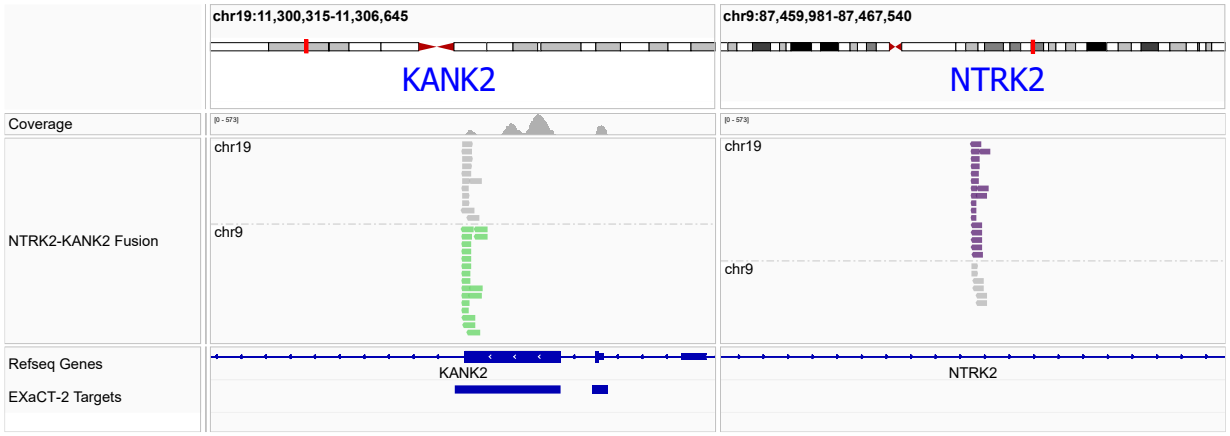

***Figure S5**: **IGV representation of the NTRK2-KANK2 fusion that was discovered by EXaCT-2.** Similar to Figure 5B, we show the reads supporting a putative fusion involving NTRK2 and KANK2. In the left-hand side of the figure, shown in green are the reads whose mate pairs align to chromosome 9, while, in the right-hand panel, reads whose mate pairs align to chromosome 9 are displayed in purple. Note, that the reads in the NTRK2 region don't align to an EXaCT-2 target region, nor an NTRK2 exon (regions shown along the bottom of the figure); while, in contrast, the reads in the KANK2 region align to a KANK2 exon boundary that is captured by the EXaCT-2 assay. rearrangement.*

Sensitivity of EXaCT-2 in detecting immunoglobulin rearrangement.

To evaluate the sensitivity of EXaCT-2 for detecting clonal rearrangements, we analyzed the HBL-1 cell line across decreasing DNA inputs (10ng, 5ng, and 1ng). We assessed all three rearrangements observed in the native HBL-1 cell line. As shown in Figure S6, the IGLV2-5/IGLJ3 clonotype was detected at 55.9% at 10ng, decreasing to 23.3% at 5ng and 3.3% at 1ng, confirming the capacity of the EXaCT-2 assay to detect clonotypes across a dynamic range. The IGKV3-20/IGKJ3 rearrangement similarly decreased with input amounts –22.9% (10ng), 10.8% (5ng), and 2.9% (1ng). Lastly, the heavy-chain rearrangement, IGHV4-34/IGHD4-17/IGHJ4 was detected at 17.6% (10 ng) and 5.9% (5 ng), but was not predominant at 1ng, though still identifiable among other rearrangements in the sample. Together, these results demonstrate that EXaCT-2 is highly sensitive, and that once a clonal rearrangement is detected, it can be tracked longitudinally as a biomarker.

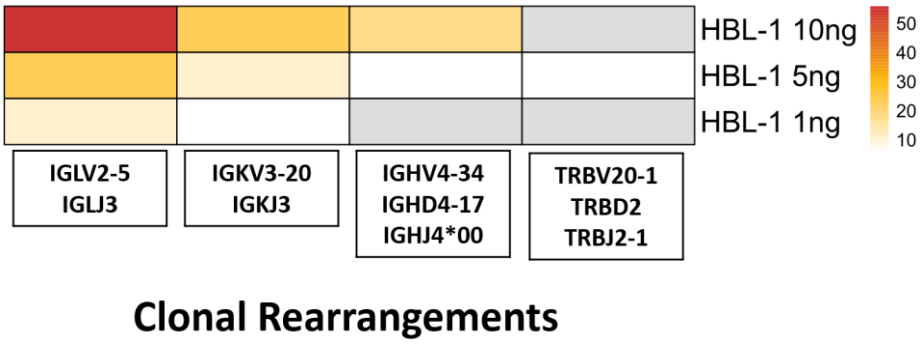

***Figure S6: Limit of detection of immunoglobulin rearrangement.** All the highlighted rearrangements in the box have a reads frequency of >= 5%. The color scheme follows the pattern depicted in Figure 3, where red indicates the highest frequency, followed by orange and then yellow. White represents the lowest frequency, while gray signifies a read frequency of 0.*

Discussion of oncogenic viruses by EXaCT-2

As described in the main text, probes for several viruses that are involved in liquid tumors and soft tissues (EBV, HTLV, KSH and MCPyV) were included in the assay design, and their capacity to detect these was tested with 14 samples from the Clinical Cohort (Table S10). Except for the MCPyV specimens – all other samples were initially identified using qualitative PCR. In contrast, the MCPyV samples were from specimens with a diagnosis of Merkel cell carcinoma (MCC) and had not undergone prior molecular testing before our analysis with the

EXaCT-2. MCC is a rare, aggressive skin cancer that is driven by either ultraviolet-induced DNA damage or MCPyV infection [4,5]. Therefore, EXaCT-2's capacity to detect MCPyV provides clinically relevant information, as it has been shown that MCPyV-negative patients are 40% more likely to experience a recurrence [6].

The EXaCT-2 assay was able to detect the presence of each virus in all positive cases and, in some instances, identified dual infections, with EBV being the most frequent co-infected virus, likely reflecting its high prevalence in the general population (Table S10). In addition to the EBV co-infections, trace amounts of KSHV and MYCPyV were also detected in samples not previously known to harbor these viruses (n = 5 and 6 coinfections, respectively, including the one negative control sample). In these incidental detections, fewer than 40 reads were mapped to these viruses, whereas positive control cases typically exceeded 1,000 reads. While this serves as a heuristic threshold, the literature does not yet define standardized read cutoffs for NGS-based viral detection, particularly given that viral genome length can influence read counts. As we expand the use of the EXaCT-2 assay, we may establish a statistically rigorous threshold. Importantly, some viruses, such as EBV, may be present in the host genome, even in low frequencies.[7–9] For this reason, we report all results to clinicians, allowing them to interpret the findings in the appropriate clinical context.

Depth of Coverage

As discussed previously, EXaCT-2 has been specifically designed to achieve increased coverage in select genomic regions crucial for cancer studies. To assess and highlight the increased coverage in these Augmented regions compared to standard regions, a set of 118 germline samples from the Discovery Cohort were analyzed across these two sets of regions. Mean Target Coverage for the different region types (augmented versus standard) was calculated by selecting the reads from the 2 target region types from the complete, deduplicated BAM files for these samples, with Mean Target Coverage calculated using the Picard CollectHsMetrics tool [10].

This analysis demonstrates that the depth of coverage provided by EXaCT-2 is robust to DNA quality, as measured by DNA Integrity Number (DIN), even in cases where samples have required DNA repair (see Methods) (Figure S7). Additionally, we provide a more detailed comparison for the clinical cohort that was used to validate the virus and fusion components of the assay as more than half of the samples (n=14/26) required FFPE repair (Figure S8).

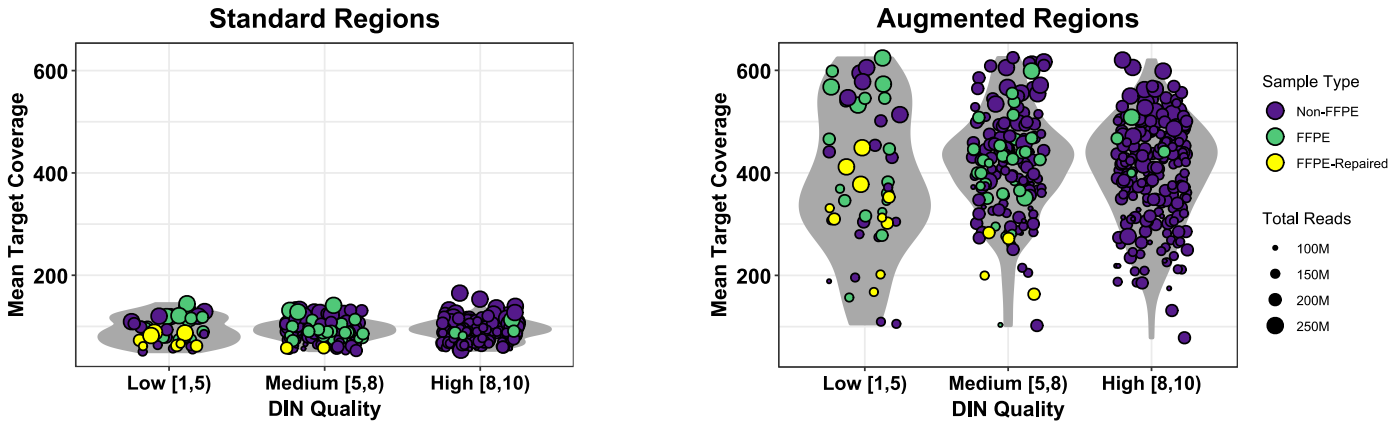

Figure S7: Comparison of mean target coverage and DNA quality, by region type (augmented vs. standard coverage) for the EIPM Discovery and Clinical cohorts. *Samples are classified by DNA Integrity Number in 3 categories: Low, Medium, and High. Left: non augmented regions; right: augmented regions. The distribution average coverage for either the augmented or standard (non-augmented) regions is not correlated to the DIN quality of the sample. FFPE and non-FFPE samples from both the Discovery and Clinical Validation Cohorts were used in this figure. FFPE samples that were repaired prior to sequencing are denoted as FFPE-Repaired (see methods, able S14 for descriptions of these cohorts). We have observed variable*

results from FFPE samples obtained from different sources. For FFPE samples with DIN < 4, we recommend using the modified protocol described in Materials and Methods.

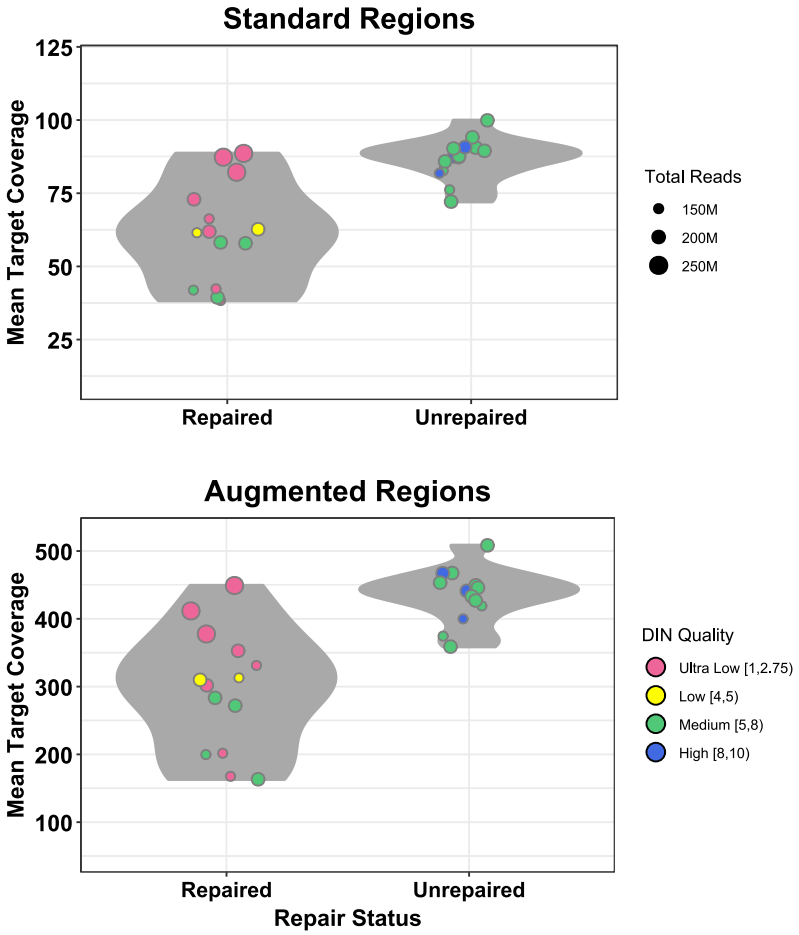

Figure S8: Comparison of Sample Coverage, based on DNA Repair Status. *This figure demonstrates the effectiveness of the DNA repair process implemented as part of the EXaCT-2 pipeline on 26 FFPE samples from the Clinical Cohort. While this figure illustrates that the process was unable to achieve coverage parity for samples requiring DNA repair, it also demonstrates that, on average, this process was capable of achieving the 300x target coverage for the augmented cancer gene regions in the samples requiring DNA repair.*

CEBPA coverage: improved coverage for GC-rich regions

Figure S9 demonstrates the far higher coverage of a region in the CEBPA gene with greater than 80% GC content. Whereas the matching EXaCT-1 sequencing for this sample only had a maximum coverage of 87 reads in the coding region, the corresponding region for this sample in EXaCT-2 had a maximum coverage of 3,506 reads from the EXaCT-2. Furthermore, there are multiple segments within the CEBPA coding region in which the EXaCT-1 assay had no or minimal (<10 reads) coverage.

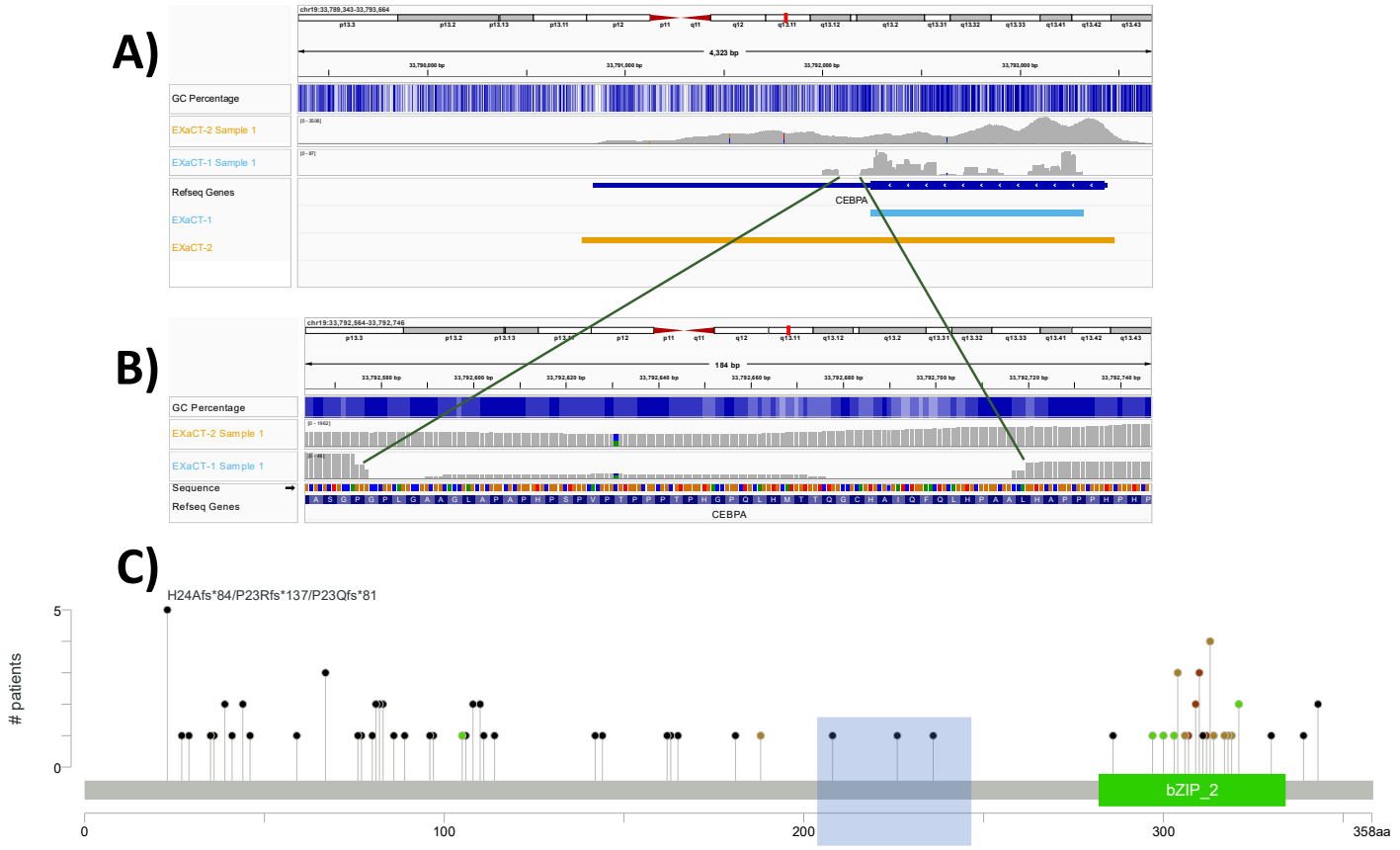

Figure S9: Enhanced coverage in high GC content regions: *A) EXaCT-2 sample has a read count of ~5400 with GC content (~80%) in CEBPA gene as compared to EXaCT-1 having a read count of ~140. B) We highlight a small segment of the CEBPA exon with extremely sparse coverage in EXaCT-1, and compare the coverage to that which was achieved with EXaCT-2. C) Lollipop plot of known mutations for CEBPA using a cohort of patients with Acute Myeloid Leukemia, collected from public sources. The GC-rich region with low coverage that is discussed in the text is highlighted in blue.*

Focusing on one such region, a GC-rich 143 nucleotide long segment that represents amino acids 201-248 in CEBPA (chr19: 33,792,577- 33,792,719), we observed that the average coverage provided by EXaCT-2 in this region for this sample was 1073 reads, whereas the maximum coverage provided by EXaCT-1 was only 17 reads, with an average of 5.5 reads and 52 positions with no coverage whatsoever (Figure S9B). Interestingly, when examining public databases of known cancer mutations in patients with Acute Myeloid Leukemia, there appears to be a sparsity of known mutations in this poorly-covered GC-rich region (n=3), suggesting that this may be a general problem for the field, regardless of the assay (Figure S9C). When the read coverage of these mutations is examined, the number of reads carrying the alternative allele is, on average, only 5.3 reads with a mean total coverage of 20 reads, indicating that even in the case of these mutations, the read support was relatively limited.

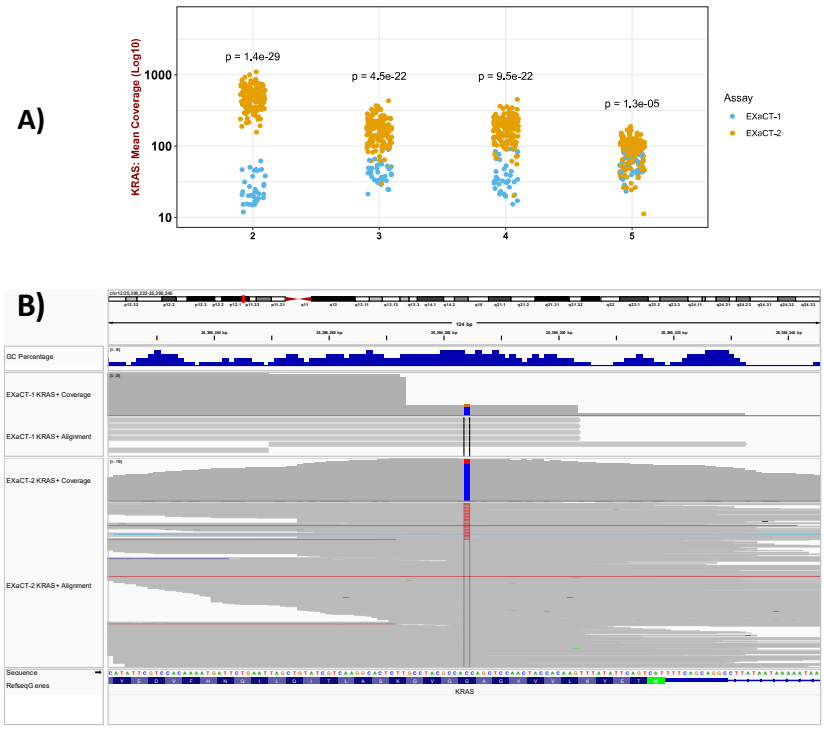

Figure S10: KRAS coverage across protein coding exons. A) *The average read coverage, per exon, of the KRAS gene is shown for samples analyzed by the EXaCT-2 assay, as well as that produced by standard WES assays, such as the EXaCT-1 assay. As shown here, exon 2, location of the well-known G12D mutation, has significantly higher coverage in EXaCT-2 compared to EXaCT-1.* ***B)*** *IGV Visualization of KRAS G12D positive samples assayed by EXaCT-1 and EXaCT-2 samples. In the top panel, we display the coverage and alignment tracks for an EXaCT-1 sample that was positive for the well-known G12D mutation, in which the coverage was only 4 total reads (with 1 carrying the alternative allele). By way of comparison, in the bottom panel, we display the coverage tracks for an unrelated G12D+ sample that was assayed by EXaCT-2. While the allele frequency in this sample was only 0.11, the number of reads with the mutant allele was 86 (out of 772 total reads covering this position).*

Figure S10A demonstrates the significantly higher coverage that we observed between the EXaCT-2 and EXaCT-1 assays for the coding exons of KRAS. To further explore this, we compared the coverage and read alignment of a $KRAS^{G12D+}$ sample that had been assayed by EXaCT-1 with that from another, unrelated $KRAS^{G12D+}$ sample that had been assayed by the EXaCT-2 assay (Figure S10B). While the EXaCT-1 assay identified this mutation, the confidence in this call was extremely low as there were only 5 total reads covering this position, with only a single read carrying the alternative allele. In comparison, with 772 total reads covering this position, with 86 reads carrying the mutant allele, the EXaCT-2 assay provides far more confidence in both the mutation call and allele frequency (0.11).

Comparison of mean target coverage for KRAS G12* mutations

We downloaded the read coverage for KRAS G12* mutations TCGA (WES and WGS) and MSK-IMPACT cohorts from cBioPortal. In total, there were 2,671 KRAS positive samples from cBioPortal and we compared with the coverage of 61 KRAS positive EXaCT-2 samples.

Comparison of VAF Distributions by Region and Platform

As described in the main text, the distribution of mutational VAFs for the EXaCT-2 assay, along with the TCGA Pan-Cancer project[11] and MSK-CHORD[12] were compared by region type. For example, the "Augmented + Problematic" panel show the VAFs for those mutations which appear in those regions that were augmented in

the EXaCT-2 assay and were classified as being problematic by the Genome In a Bottle consortium[13] along with those regions that were predicted to have a GC content greater than or equal to 80% by the UCSC Genome Browser.[14] Similarly, the "Standard Only" panel displays the VAFs of the mutations that appear in those regions that weren't predicted to be problematic, and for which the EXaCT-2 uses a standard sequencing coverage as those of other platforms. As such, the sequencing performed by the EXaCT-2 in the two "Standard" sequencing panels is most similar to that which was performed for the TCGA Pan-Cancer Project.

Note, the data for the MSK-CHORD project is completed for completeness, but as shown in Figures S11-S14, the distribution of VAFs doesn't change appreciably between the regions, which is likely due it being a high-depth, targeted panel, as opposed to the EXaCT-2 assay or the platforms used for the TCGA Pan-Cancer project.

As shown in Figures S11-S14, the VAFs of the mutations identified by EXaCT-2 assay in the regions of standard coverage display a second mode that is centered near or below 0.1 when the number of reads with supporting the alternative allele (alt reads for short) is less than 15. For example, when the minimum number of alt reads is 5, there is a sizable second mode that is centered near 0.05 (Figure S12). Similarly, when using the slightly more stringent threshold of 10, there still appears to be a small mode, centered near 0.1 (Figure S13). In contrast, the distribution of TCGA VAFs show no such secondary mode, indicating that these secondary modes in the distributions of EXaCT-2 VAFs likely stem from the inclusion of artifactual mutations.

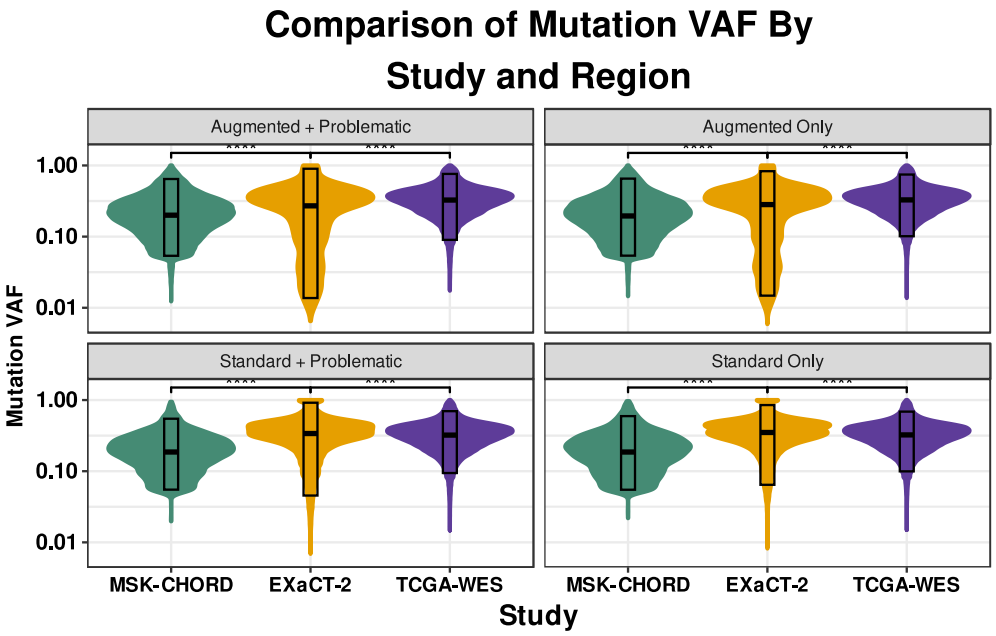

Figure S11*: Distribution of VAFs by Platform for All Mutations Supported by 15 or More Alt Reads.* *The distribution of the EXaCT-2 mutational VAFs in the regions of 'Standard' coverage closely approximates the distribution of VAFs from the TCGA. In contrast, the distributions of the EXaCT-2 mutational VAFs for the 'Augmented' regions demonstrates that the lower tails are clearly lower and broader than is reported by the TCGA, representing the far greater sensitivity offered by the EXaCT-2 platform than standard sequencing assays, even when using a minimum threshold as stringent as requiring 15 alt reads.*

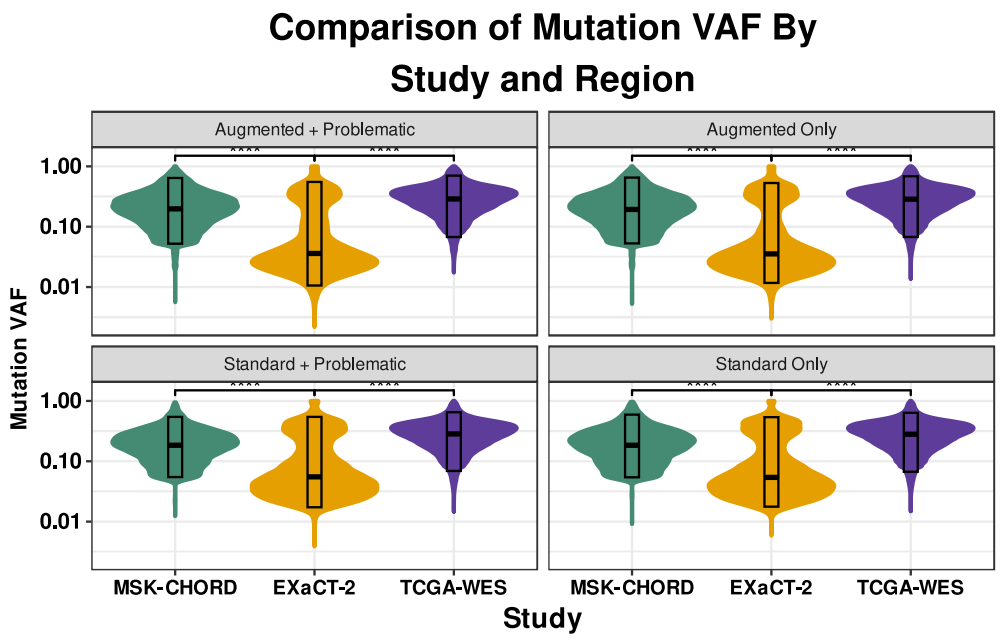

Figure S12: Distribution of VAFs by Platform for All Mutations Supported by 5 or More Alt Reads. *Unlike the distributions presented in Figure S9, there are secondary, low-VAF modes in the distribution of EXaCT-2 mutational VAFs, regardless of the region, when using a minimum alt read threshold of 5 reads. In contrast, neither the EXaCT-2 nor the TCGA-WES distributions contain these secondary, low-VAF modes. As these secondary modes appear in the regions of standard coverage, this indicates that these distributions include artifactual mutations that are potentially the result of random sequencing errors.*

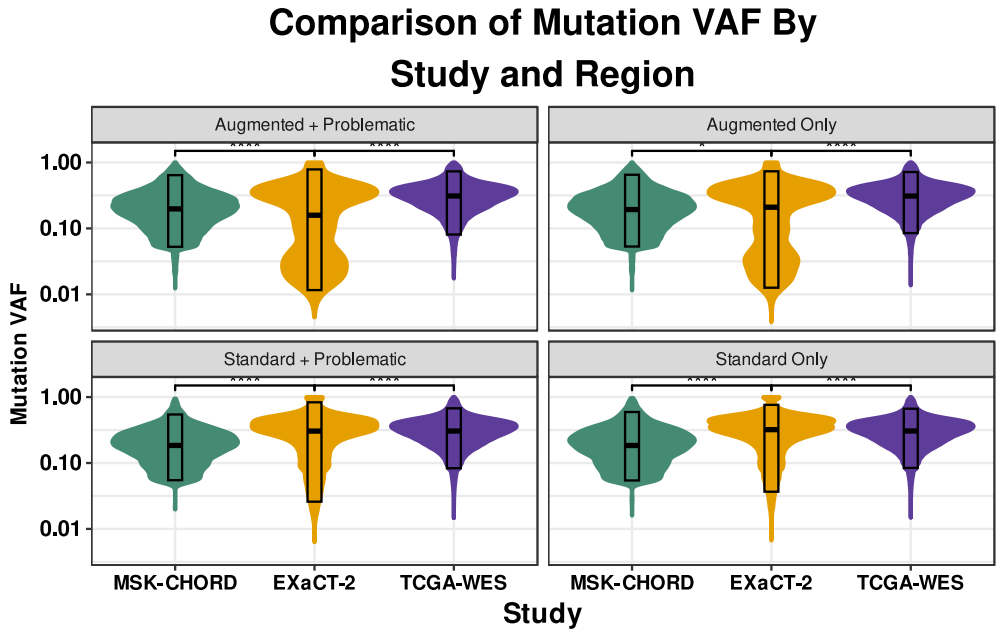

Figure S13: Distribution of VAFs by Platform for All Mutations Supported by 10 or More Alt Reads. *Unlike the distributions presented in Figure S9, when using a minimum alt read threshold of 10 reads, there are secondary, low-VAF modes in the distribution of EXaCT-2 mutational VAFs in all regions. While the secondary, low-VAF modes in the 'Standard' regions aren't as pronounced as those in Figure S10, they are clearly apparent via visual inspection, indicating that these distributions include artifactual mutations. In contrast, neither the EXaCT-2 nor the TCGA-WES distributions contain these secondary, low-VAF modes.*

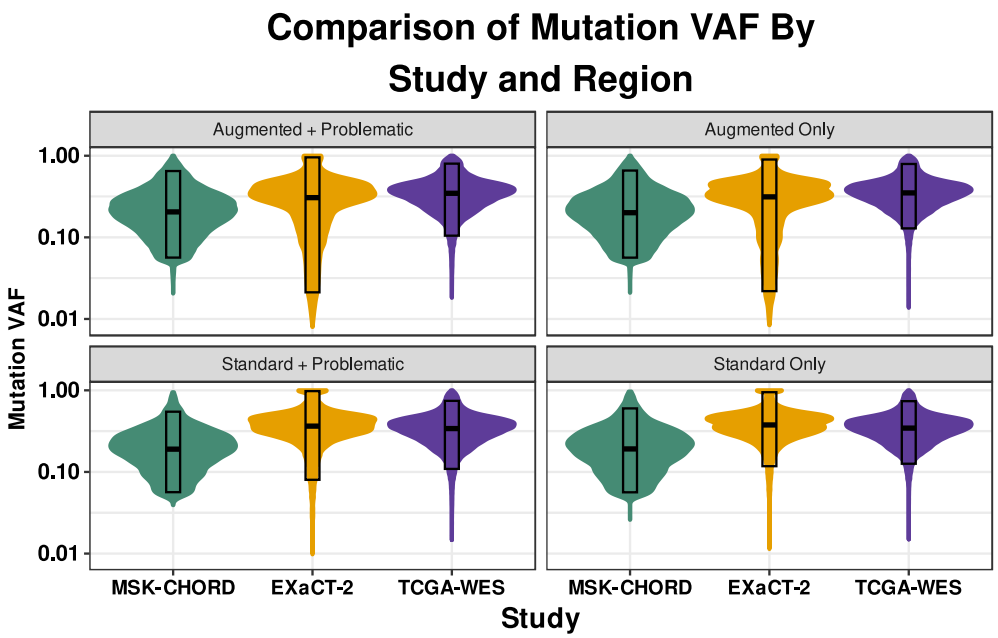

Figure S14: Distribution of VAFs by Platform for All Mutations Supported by 25 or More Alt Reads. *Included for completeness, this figure demonstrates that further increasing the minimum alt read threshold offers little further benefit to the overall distributions. However, even at this extremely stringent threshold, the broader and deeper distribution of mutational VAFs provided by the EXaCT-2 assay demonstrates that it possesses far greater sensitivity in the augmented regions than is provided by standard sequencing assays.*

Germline Analysis (Sensitivity analysis)

New York State Department of Health (NYS-DOH) requires evaluating any new NGS assay for detection of known single nucleotide polymorphisms (SNPs) and indels (sensitivity analysis). Hence, we performed this analysis using the well-characterized HapMap samples, NA12878 (n=10) and GM24385 (n=1). For this evaluation, the EXaCT-2 assay was used to collect reads from these samples, which was analyzed by the UnifiedGenotyper germline analysis tool from the Genome Analysis ToolKit (GATK)[15] version 2.5.2. Variants with a VAF lower than 35% are excluded as not representing SNPs/indels. The resulting set of SNPs and indels compared with the expected set of variants for that is provided by the Genome In A Bottle (GIAB) consortium[16]. These evaluations across all replicated 11 samples revealed an average sensitivity of 99.0% and average precision of 99.7%, indicating an exceptionally high concordance and accuracy for the EXaCT-2 and the Gold Standard set that was provided by GIAB (Table S15).

Note, regions that are categorized as FN/FP by GIAB were excluded from this analysis. These regions include highly repetitive regions, or those that are difficult to map, hence we only took into consideration the high confidence regions for our evaluation.

Assessment using clinically validated positive controls

As described in the main text, the Weill Cornell Clinical Genomics Lab applied the EXaCT-2 assay to a set of previously clinically validated samples with orthogonal methods (EXaCT-1, TSO-500, Oncomine, digital PCR; n=28) which contained clinically relevant mutations (Figure S15 and Table S16). This test achieved perfect recovery, with a high degree of concordance between the allele frequencies (Pearson correlation: 0.69; p: 5.6e-5). The greatest variations in the observed allele frequencies were associated with the mutations in difficult to assay regions, such as $KRAS^{G12+}$. As an example, the most discordant mutation we observed had a VAF from the EXaCT-1 assay of 21.4%, while the EXaCT-2 assay estimated the VAF to be over 63%. However, this difference likely stems from the difficulty of standard WES platforms, such as EXaCT-1, to assay this locus, as previously discussed. In this particular case, the EXaCT-1 assay only had access to 14 total reads from which to infer that

allele frequency, while EXaCT-2 collected a total of 724 total reads of which 460 carried the alternative allele, thereby providing far more confidence in the estimated allele frequency it generated.
In addition to these 9 mutations, 3 of these 28 clinical samples were determined to exhibit high microsatellite instability (MSI-high). This determination was made using the TruSight 500 Assay (TSO500) and its associated analytic software (Local App v2.2, using standard settings). The MSI-high status of all three samples was confirmed with the EXaCT-2 assay, using MSI-Sensor and a threshold of 0.4 (Table S17).

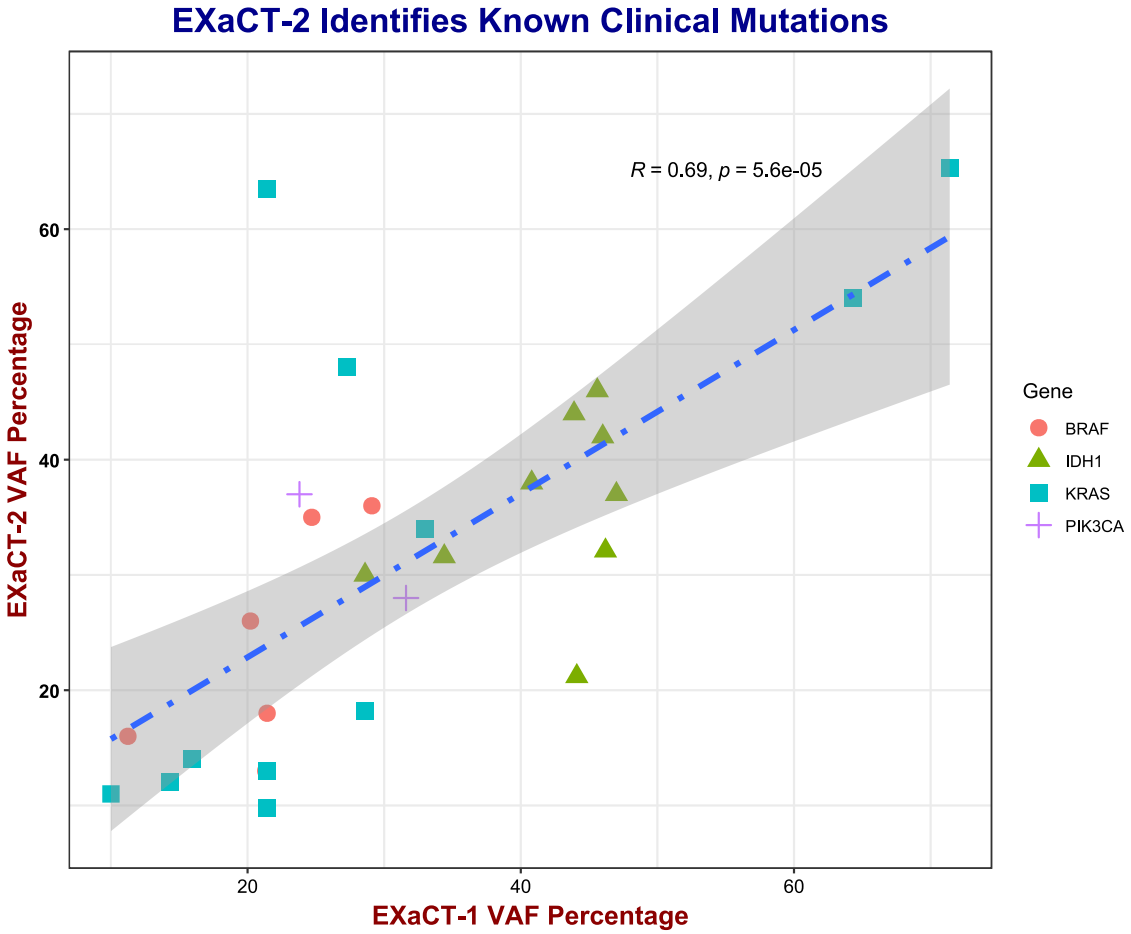

Figure S15: Comparison of the variant allele frequencies (VAFs) estimated by EXaCT-2 and EXaCT-1. *Distribution of the VAFs estimated by EXaCT-2 and EXaCT-1 for a set of known, experimentally validated and clinically-relevant mutations that were identified in a set of clinical samples. Each point represents a single mutation and the VAF that was estimated by the 2 assays.*

Customizability of the EXaCT-2 Assay: GTF2I & MTAP Genes

As part of a recently published project to explore the cancer genomes of metastatic Thymoma cancer[17], we customized the EXaCT-2 assay to improve the coverage of 2 well-known driver and marker genes for this cancer [18,19]. The improvement offered by this customization resulted in significantly improved coverage for both genes (Figure S16) relative to the baseline EXaCT-2 assay, which itself provides a considerably improved coverage than standard whole-exome-based assays such as EXaCT-1.

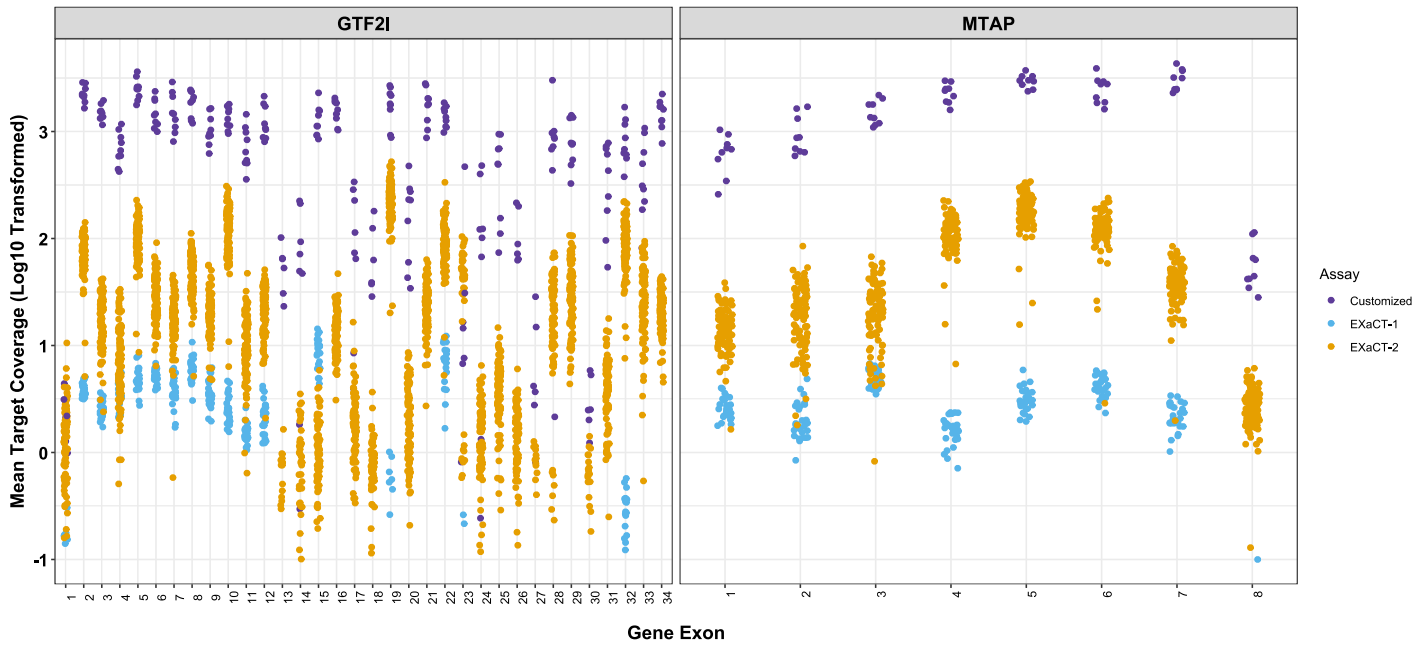

Figure S16: Enhanced Customization of GTF2I and MTAP Coverage. *This figure presents exon-level coverage for GTF2I and MTAP in samples analyzed using EXaCT-1, EXaCT-2, and a modified EXaCT-2 protocol designed to increase coverage for these genes. The standard EXaCT-2 protocol was followed, with modifications in hybridization using 5µl of EXaCT-2 Target Enrichment Human All Exon biotinylated probes, supplemented with 1µl of a custom MTAP and GTF2I probe cocktail. The customized EXaCT-2 protocol significantly improved coverage compared to both the standard EXaCT-2 and EXaCT-1 assays, which in turn outperform conventional WES methods.*

TMB in EXaCT-2 dataset compared with the TCGA

As an initial evaluation of the capacity of EXaCT-2 to evaluate Tumor Mutational Burden (TMB) and microsatellite instability (MSI), we compared the TMB between the TCGA and EXaCT-2 cohorts, stratifying by tumor of origin. For this comparison (Figure S17), TMB was calculated using a total of 106 EXaCT-2 samples and 553 TCGA samples, and to ensure for a meaningful comparison, we limited these cohorts to only include primary tumors. The EXaCT-2 cohort was comprised of 30 samples from Breast cancer, 21 from Diffuse Large B-Cell lymphoma, 6 from Pancreatic Adenocarcinoma, 31 from Lung Adenocarcinoma, and 18 from Bladder cancer (Figure S1). Similarly, the TCGA dataset was comprised of 121 cases of breast cancer, 35 cases of bladder cancer, 13 cases of pancreatic adenocarcinoma, 335 cases of lung adenocarcinoma, and 49 cases of diffuse large B-cell lymphoma.[20]

This comparison (Figure S17) indicated that Diffuse Large B-Cell Lymphoma samples exhibit nearly identical average TMB values between the 2 cohorts, while the EXaCT-2 bladder cancer samples exhibited a slightly lower, but statistically similar average TMB to the TCGA bladder samples. In contrast, the EXaCT-2 Lung Adenocarcinoma (LUAD) cohort had a statistically lower average TMB than the TCGA LUAD samples. However, for both the breast (BRCA) and pancreatic adenocarcinoma (PRAD) samples, the EXaCT-2 cohorts had a statistically higher average TMB than the TCGA cohorts. While this may appear concerning, superficially, readers should consider that these comparisons are highly imperfect given the different mutation curation and filtering schemes that were employed by the two projects, not to mention the critical differences in the assays that they employed. For example, as previously discussed, a critical feature the EXaCT-2 assay's design is improved coverage difficult-to-assay regions that were identified by previous projects, such as the TCGA.

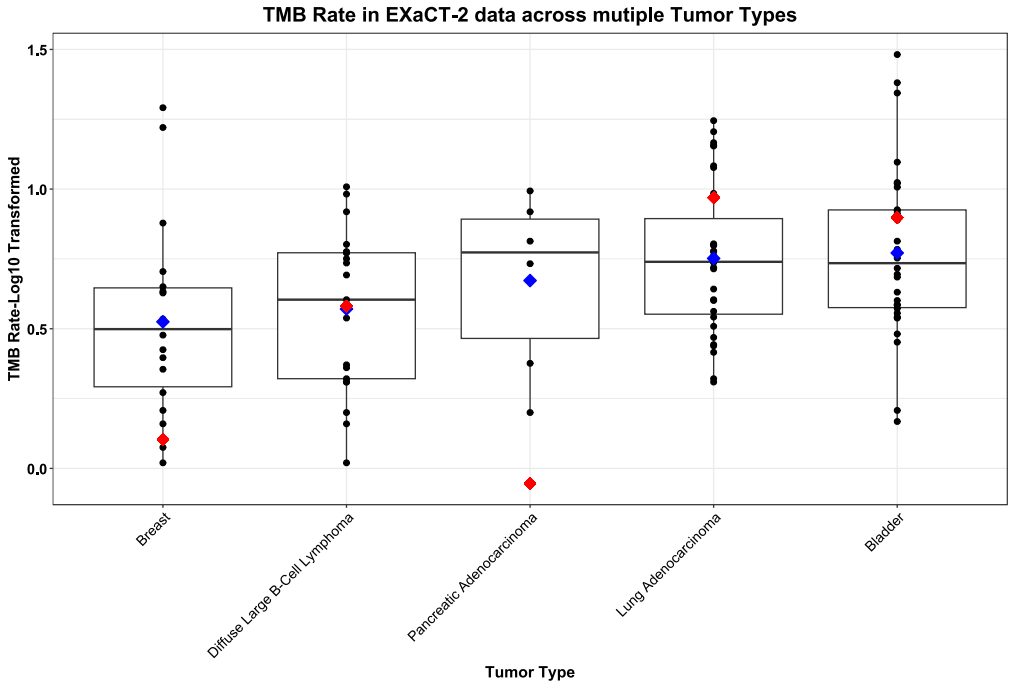

***Figure S17**: Comparing TMB from EXaCT-2 dataset to TCGA samples. Each black dot represents the TMB of an individual sample from EXaCT-2. The blue dot denotes the mean TMB across all samples within each respective tumor type from the EXaCT-2 cohort, while the red dot signifies the mean TMB across all samples from the TCGA cohort for each respective tumor type.*

TMB vs MSI in EXaCT-2 dataset

In a subsequent evaluation, we calculated the microsatellite instability (MSI) value for the 106 EXaCT-2 samples used for the TMB comparison, using MSIsensor-Pro[21]. As has been observed previously [22,23], we observed that samples having a high MSI estimate will likely also have a correspondingly higher TMB estimate; however, in contrast, high TMB status isn't associated with high MSI status (Figure S18). In these high-TMB, low-MSI cases, it has been speculated that other mechanisms drive the tumor mutational burden, including mutations of POLE [23,24].

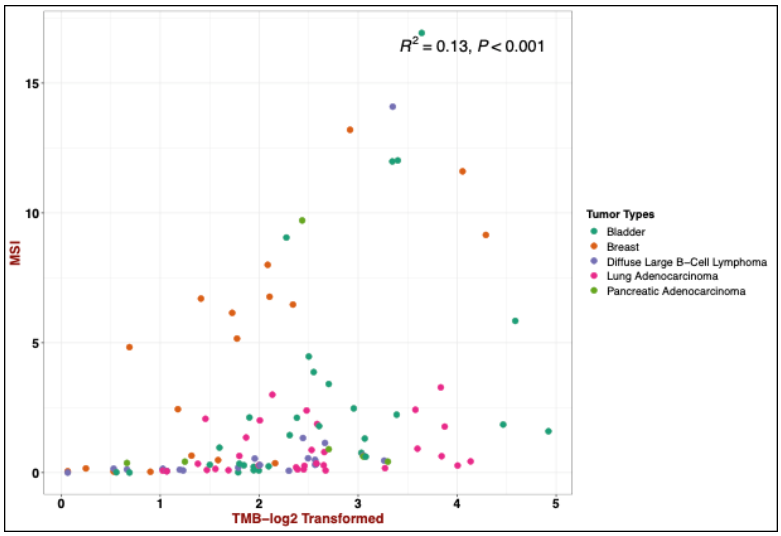

Figure S18*: TMB vs. MSI. The MSI values for the 106 samples used in Figure S17 are plotted versus the calculated TMB estimates for these samples. As has been shown elsewhere [22,23], high MSI values typically correspond to high TMB estimates, while the opposite isn't true, resulting in a weak, but still significant correlation (Pearson's R = 0.13, p-value < 0.001).*

to that specific clonotype.

Customization for complex genomic regions

Regions with high GC content

EXaCT-2 is also purposefully designed and can be tailored to achieve enhanced coverage in challenging genes that pose difficulties for various reasons. One of the potential problematic regions includes those with high GC content, such as in the case of the CEBPA gene. EXaCT-2 addresses this challenge by incorporating additional probes to cover these regions with significantly higher coverage compared to EXaCT-1. To demonstrate and substantiate this claim, we investigated the same region with high GC content (>= 80%) in the Integrative Genomics Viewer (IGV) [25] and compared the read counts in a sample from EXaCT-2 with a sample from EXaCT-1 within that region.

References

1. Venkatraman E. Seshan, A. O. DNAcopy. Bioconductor https://doi.org/10.18129/B9.BIOC.DNACOPY (2017).
2. Rennert, H. *et al.* Development and validation of a whole-exome sequencing test for simultaneous detection of point mutations, indels and copy-number alterations for precision cancer care. *NPJ Genom Med* **1**, 16019- (2016).
3. FusionGDB 2.0: fusion gene annotation updates aided by deep learning | Nucleic Acids Research | Oxford Academic. https://academic.oup.com/nar/article/50/D1/D1221/6424754.
4. Harms, P. W. *et al.* The biology and treatment of Merkel cell carcinoma: current understanding and research priorities. *Nat Rev Clin Oncol* **15**, 763–776 (2018).
5. Zaggana, E. *et al.* Merkel Cell Carcinoma—Update on Diagnosis, Management and Future Perspectives. *Cancers (Basel)* **15**, 103 (2022).
6. Paulson, K. G. *et al.* Viral oncoprotein antibodies as a marker for recurrence of Merkel cell carcinoma: A prospective validation study. *Cancer* **123**, 1464–1474 (2017).
7. Takakuwa, T. *et al.* Integration of Epstein-Barr Virus into Chromosome 6q15 of Burkitt Lymphoma Cell Line (Raji) Induces Loss of BACH2 Expression. *Am J Pathol* **164**, 967–974 (2004).
8. Reisinger, J., Rumpler, S., Lion, T. & Ambros, P. F. Visualization of episomal and integrated Epstein-Barr virus DNA by fiber fluorescence in situ hybridization. *Int J Cancer* **118**, 1603–1608 (2006).
9. Morissette, G. & Flamand, L. Herpesviruses and Chromosomal Integration. *J Virol* **84**, 12100–12109 (2010).
10. Picard Tools - By Broad Institute. https://broadinstitute.github.io/picard/.
11. Hoadley, K. A. *et al.* Multiplatform analysis of 12 cancer types reveals molecular classification within and across tissues of origin. *Cell* **158**, 929–944 (2014).
12. Jee, J. *et al.* Automated real-world data integration improves cancer outcome prediction. *Nature* **636**, 728–736 (2024).

13. Zook, J. M. *et al.* Extensive sequencing of seven human genomes to characterize benchmark reference materials. *Sci Data* **3**, 160025 (2016).
14. Perez, G. *et al.* The UCSC Genome Browser database: 2025 update. *Nucleic Acids Research* **53**, D1243–D1249 (2025).
15. Poplin, R. *et al.* Scaling accurate genetic variant discovery to tens of thousands of samples. 201178 Preprint at https://doi.org/10.1101/201178 (2018).
16. An open resource for accurately benchmarking small variant and reference calls | Nature Biotechnology. https://www-nature-com.ezproxy.med.cornell.edu/articles/s41587-019-0074-6.
17. He, Y. *et al.* Longitudinal genomic analysis of five cases of recurrent thymomas. *Journal of Thoracic Oncology* **0**, (2025).
18. Angirekula, M. *et al.* CD117, BAP1, MTAP, and TdT Is a Useful Immunohistochemical Panel to Distinguish Thymoma from Thymic Carcinoma. *Cancers (Basel)* **14**, 2299 (2022).
19. Lang, M., Kazdal, D., Mohr, I. & Anamaterou, C. Differences and similarities of GTF2I mutated thymomas in different Eurasian ethnic groups. *Transl Lung Cancer Res* **12**, 1842–1844 (2023).
20. Lawrence, M. S. *et al.* Mutational heterogeneity in cancer and the search for new cancer-associated genes. *Nature* **499**, 214–218 (2013).
21. Jia, P. *et al.* MSIsensor-Pro: Fast, Accurate, and Matched-Normal-Sample-Free Detection of Microsatellite Instability. *Genomics, Proteomics & Bioinformatics* **18**, 65–71 (2020).
22. Goodman, A. M., Sokol, E. S., Frampton, G. M., Lippman, S. M. & Kurzrock, R. Microsatellite-Stable Tumors with High Mutational Burden Benefit from Immunotherapy. *Cancer Immunology Research* **7**, 1570–1573 (2019).
23. Li, M., Gao, X. & Wang, X. Identification of tumor mutation burden-associated molecular and clinical features in cancer by analyzing multi-omics data. *Front Immunol* **14**, 1090838 (2023).
24. Hwang, H. S., Kim, D. & Choi, J. Distinct mutational profile and immune microenvironment in microsatellite-unstable and POLE-mutated tumors. *J Immunother Cancer* **9**, e002797 (2021).
25. Robinson, J. T. *et al.* Integrative Genomics Viewer. *Nat Biotechnol* **29**, 24–26 (2011).